

Sample L^AT_EX Manuscript Paper

Donald G. Luttermoser ¹
East Tennessee State University,
Department of Physics and Astronomy,
Johnson City, TN 37614

September 12, 2011

¹Visiting Astronomer, National Solar Observatory, operated by the Association of Universities for Research in Astronomy, Inc., under cooperative agreement with the National Science Foundation.

Abstract

Non-LTE calculations of semiempirical chromospheric models are presented for 30 g Her (M6 III). This star is one of the coolest ($T_{\text{eff}} = 3250$ K) SRb (semiregular) variable stars and has a mass perhaps as great as $4 M_{\odot}$. Chromospheric features we have observed in its spectrum include Mg II h & k; C II] UV0.01, which is sensitive to electron density; Mg I $\lambda 2852$; Ca II H, K & IRT; Ca I $\lambda 4227$ & $\lambda 6573$; Al II] UV1; and H α . We pay special attention to fitting the C II intersystem lines and the Mg II resonance lines but use all the other features as constraints to some extent. The equations of radiative transfer and statistical equilibrium are solved self-consistently for H I, H $^{-}$, H $_2$, He I, C I, C II, Na I, Mg I, Mg II, Al I, Al II, Ca I, and Ca II with the equivalent two-level technique. To simplify these calculations, a one-dimensional, hydrostatic, plane-parallel atmosphere is assumed.

We investigate 10 separate “classical” chromospheric models, differing most importantly in total mass column density above the temperature minimum. Synthetic spectra from these models fit some but not all of the observations. These comparisons are discussed in detail. However, we find that no single-component classical model in hydrostatic equilibrium is able to reproduce both the Mg II line profiles and the relative strengths of the C II] lines. In all these models, chromospheric emission features are formed relatively close to the star ($\lesssim 0.05 R_{\star}$). The circumstellar environment has a thick, cool component overlying the Mg II emission region, which is relatively static and very turbulent. Finally, we find that thermalization in the Mg II h & k lines in the coolest giant stars is controlled by continuum absorption from Ca I $4p^3P^{\circ}$ bound-free opacity and not collisional de-excitation as is the case for warmer K giants.

Subject headings: stars: chromospheres — stars: late-type — stars: individual (30 Hercules)

1 INTRODUCTION

In contrast to photospheres, stellar chromospheres are regions where the temperature increases with height, attaining values in the range $T_{\text{eff}} \lesssim T \lesssim 10,000$ K as the result of mechanical heating. Knowledge of the source of this mechanical heating in most stars is still preliminary in nature, but it is generally agreed that the heating probably depends on magnetic fields in main-sequence stars and giants earlier than \sim K2 (*e.g.*, Rutten 1987), while for cooler giants and supergiants, it may be accomplished by non-magnetic processes (Middelkoop 1982; Schrijver 1987), for instance by long-period (perhaps in conjunction with short-period) acoustic waves (*e.g.*, Bowen 1988; Cuntz & Stencel 1991; Ulmschneider 1991).

The chromospheres of cool stars reveal themselves through emission features of singly ionized and neutral metals in the violet and ultraviolet — especially the resonance lines of Mg II and Ca II. Mg II h and k show chromospheric emission to a greater degree than Ca II H and K because the higher abundance of ionized magnesium ensures a higher excitation rate, and because there is less photospheric continuum at the wavelength of Mg II than at Ca II in cool stars. Many lines of other common chemical elements are detected, too, although these tend to be weaker because of lower abundances (*e.g.*, Al II), unfavorable excitation potentials (*e.g.*, Si II), or complicated spectra which spread the emission over many lines (*e.g.*, Fe II). Of particular importance is the C II] UV0.01 intersystem multiplet, whose line ratios are sensitive to electron density (Stencel *et al.* 1981), and the optically thin Al II] line at $\lambda 2669$. Representative ultraviolet spectra of cool giants are given by Ayres *et al.* (1986) for α Boo (K1 III), Eaton & Johnson (1988) for several M giants, and Carpenter *et al.* (1988) for γ Cru (M3 III).

This paper represents the first attempt to form a detailed semiempirical model of the chromospheric structure of a cool ($T_{\text{eff}} < 3500$ K), oxygen-rich giant star — specifically, g Her (M6 III). Such stars represent fertile new ground for chromospheric models in that the electron density and heating mechanisms may well be different than in warmer stars. In fact, line ratios within the C II] intersystem multiplets in g Her and 2 Cen both indicate electron densities about an order of magnitude lower than in K giants (Eaton & Johnson 1988). Such cool stars are usually variable, and pulsations are thought to contribute to heating the chromospheric gas (*e.g.*, Bowen 1988; Cuntz & Stencel 1991; Eaton, Johnson, & Cadmus 1990). Indeed, it has been suggested that the structure of cool M giants may be quite different than that of K and warm M giants, with weaker chromospheres, much lower ionization of all elements, and extensive circumstellar dust formation (Stencel, Carpenter, & Hagen 1986). The mechanism of chromospheric heating, uncertain at present, may also be different in these cooler giants (Ulmschneider 1991; Dupree 1991; Cuntz & Stencel 1991).

Section 2 of this paper discusses the observations used for comparison with our theoretical models. Unlike the TX Psc model, which was based on fitting the noisy profile of only the Mg II h line and the integrated flux of C II] UV0.01, our model of g Her is derived from a multitude of high-resolution line profiles in the ultraviolet, optical, and infrared regions. Section 3 describes the procedure used in the NLTE calculations and applies them to g Her, while §4 discusses the implications of the resulting model. We conclude the paper with §5 by presenting the problems encountered with the modeling and summarizing possible solutions to the discrepancies between the synthetic and observed spectra.

Table 1: **Summary of g Her Observations**

Wavelengths	Date (U.T.)	Telescope	Camera Sequence	Resolving Power $\lambda/\Delta\lambda$	Exposure Time (<i>min</i>)
2500–3200 Å	16 June 1988	IUE	LWP 13441	500	5
2500–2900 Å	16 June 1988	IUE	LWP 13442	10,000	40
2300–3100 Å	17 June 1988	IUE	LWP 13443	10,000	880
3922–3975 Å	13 August 1989	McMath	SCCD 530	21,000	150
8488–8590 Å	14 August 1989	McMath	SCCD 547	23,000	2
4181–4248 Å	27 August 1989	McMath	SCCD 538	21,000	2
6540–6600 Å	20 April 1992	McMath	SCCD 517	45,000	5

2 OBSERVATIONS

The star 30 g Her (M6 III) is a semi-regular (SRb) variable with $V=5.04$ ($B-V=1.52$, $U-B=1.17$). Ultraviolet fluxes are barely bright enough for high-resolution, long-wavelength spectra with IUE, since the star is very inactive. The period of the star is listed as 89 days in the *General Catalog of Variable Stars* (Kukarkin *et al.* 1976), and robotic photometry over the last 6 years shows changes in visual magnitude of ~ 0.3 mag on a period of roughly this length superimposed on slower variations of close to 1.0 mag in V (Henry & Baliunas 1992). The visual spectrum is dominated by the typical TiO bands characterizing the M spectral type, but, unlike Mira variables, the star has never been reported to produce perceptible hydrogen-line emission at any phase. Its metallicity seems to be roughly solar, although carbon is depleted by a factor of two with respect to iron (Smith & Lambert 1985). It has been suggested (Smith & Lambert 1985; Judge & Stencel 1991) that g Her is an AGB (asymptotic giant branch) star from its position in the H-R diagram, a possible slight enhancement of s-process elements, and its IRAS colors (*i.e.*, AGB stars show evidence for dust; indeed, the IRAS LRS Spectral Atlas (Olson & Raimond 1986) shows g Her to have weak dust features).

The semiempirical models described here are constrained by two high-resolution IUE spectra recording the line profiles of the C II] UV0.01 intersystem lines near 2325 Å, the Mg II h and k lines near 2800 Å, and the Mg I resonance line at 2852 Å. We have also used the overall appearance of an observed low-dispersion IUE spectrum to help constrain the angular size of the star from comparisons to the synthetic spectra. Table 1 lists the the properties of the spectra used. The IUE data were reduced with the standard IUESIPS software at NASA’s Goddard Space Flight Center; we have calibrated them with the calibrations of Cassatella & Harris (1983) and Cassatella, Ponz, & Selvelli (1983). The integrated multiplet fluxes in these spectra were 6.6, 2.4, 71.8, and 2.5×10^{-13} ergs s^{-1} cm^{-2} for C II] UV0.01, Al II] UV1, Mg II UV1, and Mg I UV1, respectively. The k/h ratio for Mg II is 1.43, rather typical for K and M giants (Stencel *et al.* 1980). We have used LWP 13442 for the Mg II lines, since they were saturated in LWP 13443, and LWP 13443 for the weaker features, C II], Mg I, and Al II. Table 2 gives some useful measurements of the spectra. For the observations, we have listed integrated flux at the Earth in the Mg II h and k lines, the flux at the Earth in the lines of the C II intersystem multiplet, and the ratios of fluxes in other emission lines to Mg II. The emission line fluxes for the resonance transitions listed represent the chromospheric portion of the line (*i.e.*, the “emission cores”). For the theoretical models, we give astrophysical flux at the star, along with the same ratios.

Table 2: Integrated Fluxes in Emission Lines^a

Line	Observed ^b	T2	T3	T4	T5	T6	T7	T8	T9	T10
Mg II h&k	7.2E-12	—	896.	713.	6.96E3	1.3E5	5.89E6	7.2E4	8.05E3	1.99E4
C II λ 2324	1.1E-13	2.61	9.99	33.2	45.0	306.	7.86E4	292.	39.9	152.
C II λ 2325	3.1E-13	4.75	41.9	182.	240.	1.58E3	1.60E5	1.60E3	215.	879.
C II λ 2327	1.6E-13	3.65	22.9	88.3	124.	637.	6.37E4	664.	112.	423.
C II λ 2328	8.6E-14	2.69	10.3	34.5	46.8	318.	8.04E4	302.	41.5	158.
Line Ratios ^c										
C II]/Mg II	0.092	—	1.02	0.498	0.068	0.069	0.067	0.039	0.053	0.084
Al II/Mg II	0.033	d	d	d	d	0.024	0.021	0.025	0.023	0.034
Mg II (k/h)	1.43	—	1.94	3.46	1.83	1.79	1.49	1.83	1.88	1.79
Mg I/Mg II	0.035	—	—	—	0.045	0.023	0.050	0.028	0.038	0.029
Ca I/H α ^e	1.12	0.017	0.017	0.017	0.041	d	12.	0.059	0.031	0.72

Notes:

^a Integrated fluxes in $\text{erg s}^{-1} \text{cm}^{-2}$. An absorption line is indicated with a dash (note that all the lines for model T1 were in absorption). Also note that all fluxes for T1 through T4 are determined under the assumption of CRD. For T5–T10, resonance line fluxes are calculated with PRD.

^b Divide this column by $(5.876 \times 10^{-18})\alpha_*^2$, where α_* is the angular diameter of the star in milli-arcsec, to convert observed fluxes to model fluxes.

^c C II] \equiv C II] UV0.01; Mg II \equiv Mg II h & k; Ca II \equiv Ca II H & K; Ca I \equiv Ca I λ 6573.

^d Line not calculated for this model.

^e Ratio between the line center fluxes of these absorption lines. For model T10, this ratio gives 0.052 (no Kurucz opacities), 0.48 (Kurucz opacities included), and 0.72 (Kurucz+McMath convolution).

Figure 1 has nothing to do with this paper, I just wanted to show you how to include an encapsulated postscript file of a figure drawn in IDL into a \LaTeX file. The synthetic flux uses a compilation of bound-bound opacities described by Avrett, Machado, & Loeser (1986) which are based upon the line list of Kurucz & Peytremann (1975). It has been noted by Malagnini *et al.* (1992) that synthetic spectra based upon these older Kurucz line data reproduce the ultraviolet flux of cool stars better than the recent Kurucz line data. As a further check of the angular size of g Her, we altered the synthetic flux scale factor of our photospheric model until a best fit was obtained via a minimization of the residuals between the observed and synthetic fluxes. This fit gives an angular diameter of 28.0 mas and we have used this scale factor for our first attempts at fitting the profiles. Finally, all synthetic spectra are shifted in wavelength by the photospheric radial velocity of 3 km s^{-1} (Hoffleit 1982) for comparison with observations.

3 RADIATIVE TRANSFER CALCULATIONS

In constructing the chromospheric models, we followed the technique described by Luttermoser *et al.* (1989). First we obtain the plane-parallel, radiative-equilibrium model photosphere from the “Indiana-grid” of atmospheres with the closest match to the characteristics of g Her. For this study, we selected a model with solar abundance, $T_{\text{eff}} = 3200 \text{ K}$, and $g = 1 \text{ cm s}^{-2}$ from Brown *et al.* (1989). Since this photospheric model extends up only to a column mass m of $6.4 \times 10^{-2} \text{ g cm}^{-2}$, where the resonance lines of interest would still be very optically thick, we first extend the model

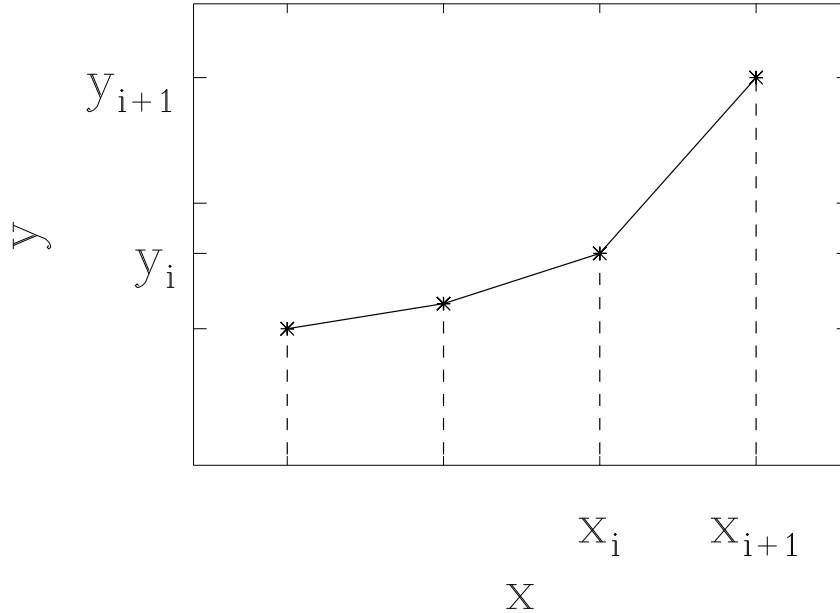


Figure 1: This figure has nothing to do with this paper. It was made with IDL procedure `sampleplot.pro`.

out to a column mass of approximately 10^{-14} g cm $^{-2}$ (see Luttermoser & Johnson 1992). Note here that we did not reconverge this extended photospheric model under the assumption of radiative equilibrium; we merely extrapolated the temperature-density gradient from the top of the published model. A synthetic spectrum calculated for this model was then used to set the flux scale factor between the observed and synthetic spectra, hence angular size of the star. We then increased the temperature as a function of height at an arbitrary depth in this extended photosphere to simulate a chromosphere. For all these calculations, we initially assumed a low microturbulent velocity of 3 km s $^{-1}$ throughout the atmosphere, roughly the photospheric value (Smith & Lambert 1985; Tsuji 1991).

Because the ionization and excitation in chromospheric gases may depart wildly from the predictions of LTE (local thermodynamic equilibrium), a self-consistent solution to the coupled equations of statistical equilibrium and radiative transfer are required for a model atom of the species to be considered. These calculations were performed with the radiative transfer code PANDORA (*e.g.*, Vernazza, Avrett, & Loeser 1973 (VAL I), 1978 (VAL II), 1981 (VAL III); Avrett & Loeser 1992) in a horizontally homogeneous, plane-parallel geometry. Under these assumptions, the radiative transfer equation is written as,

$$\mu \frac{dI_\nu}{d\tau_\nu} = I_\nu - S_\nu, \quad (1)$$

where parameters above have their usual meaning, and the quantities shown include all processes (continuum and line) taking place at that frequency. Statistical equilibrium is formulated as

$$n_i \sum_{j=1(\neq i)}^N [P_{ij} + P_{i\kappa}] = \sum_{j=1(\neq i)}^N [n_j P_{ji} + n_\kappa P_{\kappa i}] \quad (2)$$

and

$$n_\kappa \sum_{i=1}^N P_{\kappa i} = \sum_{i=1}^N n_i P_{i\kappa}, \quad (3)$$

where n_i represents the number density in bound level i (up to a maximum of N levels in the representative atomic model), n_κ represents the continuum (*i.e.*, ion) number density, and P represents the total transition rate (radiative R plus collisional C) between the respective states. Equations (1)-(3) are solved iteratively with the equivalent two-level approach. With this method, emission and absorption of photons in a line are expressed in terms of a net radiative bracket ρ_{ji} defined by the net radiative rate equation

$$n_j A_{ji} \rho_{ji} = n_j (A_{ji} + B_{ji} \bar{J}_{ji}) - n_i B_{ij} \bar{J}_{ji}, \quad (4)$$

where A_{ji} , B_{ji} , and B_{ij} are the Einstein coefficients for spontaneous emission, stimulated emission, and absorption respectively, and \bar{J} is the total mean intensity integrated over the normalized absorption coefficient in the ji transition. It can be shown that the line source function can be written as

$$S_{ji} = \frac{2h\nu_{ji}^3/c^2}{(g_j/g_i)(n_i/n_j) - 1}, \quad (5)$$

and the net radiative bracket as

$$\rho_{ji} = 1 - \frac{\bar{J}_{ji}}{S_{ji}}, \quad (6)$$

where g represents the statistical weight of the level.

We calculated the line profiles for 10 separate chromospheric temperature distributions resembling “classical” chromospheric models – a rapid rise in temperature at the top of the photosphere followed by a linear increase in temperature as a function of column mass to some maximum value near 10,000 K at the top of the chromosphere. Properties of all ten models are given in Table 3. Our first chromosphere (T1) introduced a temperature rise at $T = 2119$ K and $\log m = -1.23$ (or $z = -1.52 \times 10^7$ km, where z increases into the star, and $z = 0$ corresponds to $\tau[5000 \text{ \AA}] = 1$) with a linear temperature increase with respect to $\log m$ up to the top of the model, where $T = 12,000$ K at $\log m = -13.9$ ($z = -1.85 \times 10^8$ km). This model was unsatisfactory in that it produced pure absorption features for Mg I UV1, Mg II h & k, Ca II H & K, and C II] UV0.01. We next enhanced the temperature in the lower chromosphere ($-9.34 < \log m < -1.68$ [g cm^{-2}] or $-1.02 \times 10^8 < z < -1.70 \times 10^7$ km) by an average of 1000 K (chromosphere T2). The temperature enhancement at the base of the chromosphere increased the pressure scale height, which in turn expanded the top of the chromospheric model out to -2.21×10^8 km. This model produced weak C II] features with an integrated flux at Earth of 1.6×10^{-14} ergs $\text{s}^{-1} \text{cm}^{-2}$ (for an angular diameter of 28 mas). Our resonance lines of interest remained pure absorption features.

4 DISCUSSION

Because of discrepancies among the results for C II], Mg II, and H α , we have been unable to fit even the best available chromospheric diagnostics with a single plane-parallel, hydrostatic, homogeneous *classical* chromospheric model. These discrepancies had the following form: In order to get the electron density high enough with a traditional model, the lines must form at such high mass column density that H α becomes much too strong, some photospheric lines develop unobserved emission cores, and the wings of Mg II h and k become much too broad. Other discrepancies include the ratios of emission lines. While C II], Al II], Mg II, and Mg I are formed in roughly the

Table 3: Chromospheric Models Considered

Model	T_{min}^a	$\log m_{min}^a$	T_{knee}^b	$\log m_{knee}^b$	$n_e(\text{C II])}^c$	$H \text{ (km)}^d$
T1	2119	-1.23	—	—	—	1.70×10^8
T2	2119	-1.23	3500	-1.68	2.9×10^6	2.06×10^8
T3	2140	-0.92	5500	-2.28	9.3×10^6	2.21×10^8
T4	2140	-0.92	6200	-2.28	8.9×10^6	2.31×10^8
T5	2156	-0.70	6800	-2.28	1.6×10^7	2.35×10^8
T6	2264	-0.03	5800	-1.23	9.1×10^6	1.67×10^8
T7	2426	0.68	6920	-1.23	1.2×10^9	2.16×10^8
T8	2223	-0.25	6200	-1.68	9.1×10^7	2.02×10^8
T9	2156	-0.70	6800	-2.28	1.4×10^7	2.45×10^8
T10	2156	-0.70	7000	-2.28	3.4×10^7	2.23×10^8

Notes:

- ^a Temperature (in K) and the logarithm of the column mass (in g cm^{-2}) of the atmospheric position that separates the photosphere from the chromosphere.
- ^b Temperature (in K) and the logarithm of the column mass (in g cm^{-2}) of the atmospheric position where the chromospheric temperature profile flattens.
- ^c Electron density (in cm^{-3}) at the depth of formation of the C II] UV0.01 features.
- ^d Thickness of the chromosphere (in km) from the temperature minimum to the outermost region.

same part of the chromosphere, the emission portion of the Mg I and Mg II features form over a range from $4.7 \times 10^{-4} \leq m \leq 5.9 \times 10^{-2} \text{ g cm}^{-2}$ and $3.5 \times 10^{-6} \leq m \leq 27 \text{ g cm}^{-2}$ respectively. Indeed, the peak flux of the Mg I and Mg II line originate from the same depth ($m = 2.1 \times 10^{-2} \text{ g cm}^{-2}$) as the formation depths of the C II] and Al II] emission lines and the core of H α . This coincidence arises quite naturally in this one-dimensional, hydrostatic modeling, for we need to find a temperature rise to produce both Mg II and Mg I emission. If we raise the temperature too far out, the density is too low for Mg I to have sufficient opacity for emission features to form at the typical chromospheric temperatures (*i.e.*, 5000-7000 K), whereas Mg II still possesses sufficient opacity, due to its slightly higher number density at these temperatures as compared to Mg I, to produce emission. We cannot start the temperature rise too deep since observed “photospheric” absorption lines (*i.e.*, Mg I $\lambda 4571$) go into emission. Due to these constraints, the temperature rise must begin around $m = 0.1 - 0.3 \text{ g cm}^{-2}$ and increase dramatically to temperatures between 5000-7000 K at around 0.02 g cm^{-2} . Such a sharp temperature rise suggests that a shock structure may exist in this region of the atmosphere.

4.1 Electron Densities

The observed C II] line ratios indicate the electron density should be increased in our model by an order of magnitude. The hydrogen density is quite low at the formation depth of these lines, and one would have to increase the temperature at this depth to well over 10,000 K to produce the observed ratios. This, of course, would produce enormous Balmer emission lines (as seen in Mira variable stars) which have not been seen in this star. This discrepancy can also be remedied by moving the chromosphere in to lower depths, but then one runs into the problems mentioned above. There is the possibility that the C II] ratios are unrepresentative of this star because of noise in the IUE spectra near 2325 Å (GHRS observations of these very cool giants would be invaluable), but the appearance of this multiplet here is very similar to that in the M5 III star 2 Cen (Eaton & Johnson 1988), the only other M giant this cool observed in the C II] lines. At the formation depth of the C II] lines and the peak flux of the Mg II lines, H I contributes 64.0% of the electrons followed by O I (20.6%), C I (8.5%), Ne I (1.1%), and N I (1.0%). Both hydrogen and carbon are handled in NLTE, while the rest are in LTE. Carbon is 96.8% ionized at this depth and $n_{\kappa}/n_{\kappa}^* \approx 1$, indicating that we cannot increase the electron density at these depths with carbon. Hydrogen is 64% ionized at this region and is severely underionized with respect to LTE (~ 3 orders of magnitude). Luttermoser & Johnson (1992) have shown that the Lyman lines act as a *drain* in the chromosphere of late-type giants and that PRD gives the same level/ion densities as CRD at these depths. Hence, we cannot enhance the electron density at this region of the atmosphere from a better treatment of hydrogen (*i.e.*, including more levels will slightly enhance the Lyman-line drain). One might expect oxygen to have similar ionization properties as hydrogen, since it has nearly the same ionization potential and has strong UV resonance lines. Radiative transfer in the oxygen atom is very complicated however. Field & Steigman (1971) have shown that the charge-exchange reaction $\text{O} + \text{H}^+ \Leftrightarrow \text{O}^+ + \text{H}$ can dominate the ionization equilibrium of oxygen in low density environments. This charge-exchange reaction for our model in the Mg II emission region would give $n(\text{O}^+)/n(\text{O}) \approx \frac{9}{8}n(\text{H}^+)/n(\text{H})$ — oxygen underionized with respect to LTE which would substantially reduce the electron density. Haisch *et al.* (1977), however, have shown the importance of the Ly β -pumped fluorescence mechanism to the excitation of the 1302–1306 Å resonance lines of the O I atom. The $^3P_2 - ^3D$ excitation at 1025.77 Å via Ly β photons, followed by an immediate ionization out of the 3D state from the intense far-IR photospheric radiation field of this star, might give rise to an overionization of O I with respect to

LTE. Such a mechanism could enhance the electron density in the lower chromosphere and rectify the C II] line ratio problem; however, Carlsson & Judge (1993) have determined that this scenario will not work. Unfortunately, we cannot further test this mechanism since such a calculation involving fluorescence is currently not possible with PANDORA. The likely explanation to the electron density discrepancy probably involves our omission of hydrodynamic processes, which will enhance the gas density at these depths, and possible inhomogeneities in the atmospheric structure (see Ayres 1990; Jørgensen & Johnson 1991; and Wiedemann & Ayres 1991). Finally, an increase in the surface gravity by an order of magnitude would help to rectify this problem.

4.2 Ca II H & K

The chromospheric emission features in the Ca II H & K line cores of g Her (and most cool giant stars) are observed to be too weak relative to Mg II h & k. From this study, we can identify several reasons for this inconsistency. (1) The thermalization of photons scattering in the line wings is dominated by collisional de-excitation (*i.e.*, depth-dependent PCS) instead of continuum processes (*i.e.*, depth-independent PCS) as was the case for the Mg II lines. This results in the Ca II chromospheric emission flux being weaker and broader than would be the case for depth-independent PCS. (2) The enhanced microturbulent velocity in the lower chromosphere further broadens the Ca II emission, depressing the peak flux further. (3) Boesgaard & Hagen (1979) have also suggested that the weakness could further be the result of increased attenuation in a wind that absorbs over the entire range of velocity of the Ca II emission features. We do not place too much weight on this suggestion, since it is difficult to understand why a large velocity gradient presents itself in the formation region of the Ca II cores (*i.e.*, the H₃ and K₃ features) and is not evident in the Mg II line cores which are formed slightly higher in the atmosphere. Instead, we simply claim that the chromospheric velocity field shifts the K₃ and H₃ features slightly blueward to help hide some of the chromospheric emission. (4) We also need to rely on overlying absorption from neutral metals to explain the weakness of the features.

5 CONCLUSIONS

Luttermoser & Johnson (1992) have already described the difficulties in carrying out NLTE calculations in cool, low density, stellar atmospheres and the techniques one must use to converge a solution using the equivalent two-level approach. Since one must attempt to fit as many *chromospheric indicators* as one can access, many runs must be made for each atom and ion handled in NLTE. We have obtained a large number of observational constraints for g Her to carry out this analysis and have found that semiempirical techniques involving “classical” models under the assumptions of one-dimensional, homogeneous geometries in hydrostatic equilibrium cannot reproduce all of the spectral features of this star. We note here that we have begun to carry out preliminary calculations of a g Her model with similar characteristics to hydrodynamic models of Mira variables (*i.e.*, a model with a permanent chromosphere, or “calorisphere,” and outward propagating shocks, see Bowen 1988). We will show in a subsequent paper that many of the “chromospheric” spectral features of this semiregular variable can be reproduced with such a model. This suggests that future modeling of these late-type variable stars, both the Miras and semiregulars, require atmospheric

modeling with dynamic processes (see Bowen 1988) and possibly inhomogeneous geometries (see Jørgensen & Johnson 1991) included in the calculations. Previous semiempirical chromospheric models of late-type giants, based on a limited set of spectral features (*e.g.*, the model for TX Psc by Luttermoser *et al.* 1989), are not true representations of the thermal structure of these stellar atmospheres.

This investigation leads to the following conclusions. (1) The chromospheric structure of semiregular, late-type giant stars (g Her as the prototype) cannot be described by the classical, one-component model in hydrostatic equilibrium. (2) Inconsistencies between ultraviolet emission features and infrared CO absorption suggest the outer atmosphere of these stars are inhomogeneous. (3) Such inhomogeneities, however, cannot account for the difficulty in fitting both the C II] intersystem line ratios and the Mg II profiles — we suggest that hydrodynamic processes (*i.e.*, shocks) may help resolve this problem. (4) Thermalization in the Mg II h & k lines in cool giant stars is controlled by continuum absorption and not collisional de-excitation as is the case for warmer K giants. (5) The chromospheric emission features (*i.e.*, UV emission features) seen in these stars are formed relatively close to the star ($r \lesssim 0.05R_\star$). (6) The circumstellar environment includes a cool component that resides above the chromosphere, which is relatively static and very turbulent with a hydrogen column mass of $\sim 3 \times 10^{20} \text{ cm}^{-2}$.

We thank Mr. Dave Jaksha of the National Solar Observatory for showing us how to use the McMath solar telescope and stellar spectrograph and for help with the preliminary data reductions of our ground-based observations. We thank Dr. Frederick Walter for help in reading FITS-formatted tapes, and Drs. Eugene Avrett and Rudolf Loeser for encouraging us to use their PANDORA stellar atmospheres code. Thanks are also extended to Dr. Philip Judge for helpful discussions and useful comments on the manuscript, and to an anonymous referee for additional comments. Finally, we wish to thank Drs. Sallie Baliunas, Louis Boyd, Russell Genet, and Greg Henry for the photometric results of g Her, which were obtained with the Smithsonian 0.25m APT, operated jointly by the Smithsonian Astrophysical Observatory, Fairborn Observatory, and Tennessee State University and generously supported by SAO Director Dr. Irwin Shapiro. Use of the Colorado IUE-RDAF, supported by NASA contract NAG 5-28731, is acknowledged. This research was partially supported by NASA grants NAG 5-1181 and NAG 5-1777 to Iowa State University; NAG 5-1305 to the University of Colorado; NAG 5-182 to Indiana University; and NAG 5-1327 to East Tennessee State University.

REFERENCES

- Avrett, E.H., & Loeser, R. 1984, in *Methods in Radiative Transfer*, ed. W. Kalkofen (Cambridge: Cambridge University Press), 341
- 1992, in *Seventh Cambridge Workshop on Cool Stars, Stellar Systems, and the Sun*, eds. M.S. Giampapa & J.A. Bookbinder (ASP Conf. Ser. 26), 489
- Avrett, E.H., Machado, M.E., & Loeser, R. 1986, in *The Lower Atmosphere in Solar Flares*, ed. D.F. Neidig (Sunspot, NM: National Solar Observatory), 216
- Ayres, T.R. 1990, in *Sixth Cambridge Workshop on Cool Stars, Stellar Systems, and the Sun*, ed. G. Wallerstein (ASP Conf. Ser. 9), 106

- Ayres, T.R., Judge, P., Jordan, C., Brown, A., & Linsky, J.L. 1986, *ApJ*, 311, 947
- Boesgaard, A.M., & Hagen, W. 1979, *ApJ*, 231, 128
- Bowen, G.H. 1988, *ApJ*, 339, 299
- Brown, J.A., Johnson, H.R., Alexander, D.R., Cutright, L., & Sharp, C.M. 1989, *ApJS*, 71, 623
- Carlsson, M., & Judge, P.G. 1993, *ApJ*, 402, 344
- Carpenter, K.G., Pesce, J.E., Stencel, R.E., Brown, A., Johansson, S., & Wing, R.F. 1988, *ApJS*, 68, 345
- Cassatella, A., & Harris, A.W. 1983, *NASA IUE Newsletter*, No. 23, 21
- Cassatella, A., Ponz, D., & Selvelli, P.L. 1983, *NASA IUE Newsletter*, No. 21, 46
- Cuntz, M., & Stencel, R.E. 1991, in *Mechanics of Chromospheric & Coronal Heating*, ed. P. Ulmschneider, E.R. Priest, R. Rosner (Berlin: Springer), 206
- Dupree, A.K. 1991, in *Mechanics of Chromospheric & Coronal Heating*, ed. P. Ulmschneider, E.R. Priest, R. Rosner (Berlin: Springer), 185
- Eaton, J.A., & Johnson, H.R. 1988, *ApJ*, 325, 355
- Eaton, J.A., Johnson, H.R., & Cadmus, R.R. 1990, *ApJ*, 364, 259
- Field, G.B., & Steigman, G. 1971, *ApJ*, 166, 59
- Haisch, B.M., Linsky, J.L., Weinstein, A., & Shine, R.A. 1977, *ApJ*, 214, 785
- Henry, G., & Baliunas, S.L. 1992, private communication.
- Hoffleit, D. 1982, *The Bright Star Catalogue* (New Haven: Yale Univ. Obs.)
- Jørgensen, U.G., & Johnson, H.R. 1991, *A&A*, 244, 462
- Judge, P.G., & Stencel, R.E. 1991, *ApJ*, 371, 357
- Kukarkin, B.V., Kholopov, P., Efremov, Y.U., Kukarkina, N.P., Kuruchkin, N.E., Medvedeva, G.I., Perova, N.B., Federovich, V.P., and Frolov, M.S., 1976, *General Catalog of Variable Stars, 3rd Supplement* (3rd Ed.; Moscow: Akad. Nauk)
- Kurucz, R.L., & Peytremann, E. 1975, *Smithsonian Astrophys. Obs. Rep.* No. 362
- Luttermoser, D.G. 1988, Ph.D. Thesis, Indiana Univ.
- . 1993, in preparation
- Luttermoser, D.G., Bowen, G.H., Willson, L.A., & Brugel, E.W. 1993, in preparation
- Luttermoser, D.G., & Johnson, H.R. 1992, *ApJ*, 388, 579
- Luttermoser, D.G., Johnson, H.R., Avrett, E.H., & Loeser, R. 1989, *ApJ*, 345, 543
- Malagnini, M.L., Morossi, C., Buser, R., & Parthasarathy, M. 1992, *A&A*, 261, 558
- Middelkoop, F. 1982, *A&A*, 113, 1

- Olson, F.M., & Raimond, E. 1986, A&AS, 65, 607
- Rutten, R.G.M. 1987, A&A, 177, 131
- Schrijver, C.J. 1987, A&A, 172, 111
- Smith, V.V., & Lambert, D.L. 1985, ApJ, 294, 326
- Stencel, R.E., Carpenter, K.G., & Hagen, W. 1986, ApJ, 308, 859
- Stencel, R.E., Linsky, J.L., Brown, A., Jordan, C., Carpenter, K.G., Wing, R.F., & Czyzak, S. 1981, MNRAS, 196, 47P
- Stencel, R.E., & Mullan, D.J. 1980, ApJ, 238, 221
- Stencel, R.E., Mullan, D.J., Linsky, J.L., Basri, G.S., & Worden, S.P. 1980, ApJS, 44, 383
- Tsuji, T. 1991, A&A, 245, 203
- Ulmschneider, P. 1991, in Mechanics of Chromospheric & Coronal Heating, ed. P. Ulmschneider, E.R. Priest, R. Rosner (Berlin: Springer), 328
- Vernazza, J.E., Avrett, E.H., and Loeser, R. 1973, ApJ, 184, 605 (VAL I)
- . 1976, ApJS, 30, 1 (VAL II)
- . 1981, ApJS, 45, 635 (VAL III)
- Wiedemann, G., & Ayres, T.R. 1991, ApJ, 366, 277